TOXICOLOGICAL SCIENCES **104(2)**, 405–411 (2008)
doi:10.1093/toxsci/kfn089
Advance Access publication May 7, 2008

Mitogen-activated Protein Kinase Kinase Kinase 1 Protects against Nickel-induced Acute Lung Injury

Maureen Mongan,*,[2] Zongqing Tan,*,[2] Liang Chen,* Zhimin Peng,* Maggie Dietsch,* Bing Su,† George Leikauf,*,‡ and Ying Xia*,[1]

Department of Environmental Health and Center of Environmental Genetics, University of Cincinnati, School of Medicine; †Department of Immunobiology, Yale University School of Medicine; and ‡Department of Environmental and Occupational Health, Graduate School of Public Heath, University of Pittsburgh

Received March 11, 2008; accepted April 29, 2008

Nickel compounds are environmental and occupational hazards that pose serious health problems and are causative factors of acute lung injury. The c-jun N-terminal kinases (JNKs) are regulated through a mitogen-activated protein (MAP) 3 kinase-MAP2 kinase cascade and have been implicated in nickel toxicity. In this study, we used genetically modified cells and mice to investigate the involvement of two upstream MAP3Ks, MAP3K1 and 2, in nickel-induced JNK activation and acute lung injury. In mouse embryonic fibroblasts, levels of JNK activation and cytotoxicity induced by nickel were similar in the *Map3k2*-null and wild-type cells but were much lower in the *Map3k1*/*Map3k2* double-null cells. Conversely, the levels of JNK activation and cytotoxicity were unexpectedly much higher in the *Map3k1*-null cells. In adult mouse tissue, MAP3K1 was widely distributed but was abundantly expressed in the bronchiole epithelium of the lung. Accordingly, MAP3K1 ablation in mice resulted in severe nickel-induced acute lung injury and reduced survival. Based on these findings, we propose a role for MAP3K1 in reducing JNK activation and protecting the mice from nickel-induced acute lung injury.

Key Words: **MAP3K; MAP2K; MAPK; JNK; acute lung injury; nickel cytotoxicity.**

Nickel compounds, having extensive usage in industry, are present in welding fumes and are components of ambient particulate matter released from coal-fired power plants (Lippmann *et al*., 2006). Welders and other workers exposed to nickel-containing materials can develop a variety of adverse health problems, particularly of the respiratory system (Antonini *et al*., 2003; Speizer, 2000). Nickel inhalation is associated with acute lung injury in humans that can lead to respiratory failure, clinically characterized as diffuse alveolar damage, inflammatory cell influx and activation, insufficient gas exchange, and ultimately death (Scott *et al*., 2002). Although a large number of people develop acute lung injury, only a fraction succumb to respiratory failure, suggesting that genetic variability may determine the patient's risk and subsequent outcome of acute lung injury.

Acute lung injury is caused by respiratory epithelial cell damage and loss of function. The initial tissue injury triggers the production of growth factors, extracellular matrices, and cytokines, which, through the activation of a series of intracellular signaling pathways, stimulate inflammatory responses and migration and proliferation of pulmonary epithelial cells (Geiser *et al*., 2000; Kheradmand *et al*., 1994). Signaling pathway activation, on the one hand, promotes re-epithelialization of the damaged epithelium thereby restoring normal barrier function, while on the other hand, contributes to pathological damage, such as inflammation, disruption of surfactant homeostasis, and fibrosis. Thus, gene-environment interactions affecting the efficiency of signal transduction may influence the development and severity of acute lung injury.

The mitogen-activated protein kinases (MAPKs), including the c-jun N-terminal kinase (JNK) (also known as MAPK8), the extracellular signal-regulated kinase (ERK1/2 also known as MAPK1/3), and the p38s (also known as MAPK14), play a pivotal role in the transmission of extracellular signals through the cytosol to the nucleus. The MAPK activation is mediated by a cascade involving a mitogen-activated kinase kinase kinase (MAP3K)-MAPK kinase (MAP2K) module, where extracellular signals first activate the MAP3K leading to the phosphorylation of MAP2K, which in turn phosphorylates and activates MAPKs (Davis, 2000). Once activated, the MAPKs can translocate to the nucleus, where they phosphorylate transcription factors, therefore converting transient biochemical signals to permanent changes of gene expression. Through this paradigm, MAPKs participate in numerous physiological and pathological processes, such as immunity, neuronal development, and cancer (Chang *et al*., 2003; Chen *et al*., 2001; Dong *et al*., 1998; Han *et al*., 2002; Kuan *et al*., 1999; Sabapathy *et al*., 2001).

[1] To whom correspondence should be addressed at Department of Environmental Health, University of Cincinnati, 3223 Eden Avenue, Cincinnati, OH 45267-0056. Fax: (513) 558-0974. E-mail: xiay@email.uc.edu.

[2] These authors contributed equally to this work.

The role of JNK activation in lung injury is controversial and yet to be fully understood. *In vitro*, lung injury inducers, including metals, mechanical ventilation, and inflammatory cytokines, can activate the JNK MAPK, specifically in human dendritic cells and in airway and alveolar epithelial cells (Boisleve *et al*., 2004; Sakashita *et al*., 2007; Timblin *et al*., 1998). The JNK activation in turn is connected to physiopathological responses in the lung, such as epithelial cell proliferation and tumorigenesis (Timblin *et al*., 1998), cell apoptosis, neutrophil chemotaxis (Li *et al*., 2004; Sakashita *et al*., 2007), and inflammatory gene expression (Han *et al*., 2005). *In vivo*, pharmacologic inhibition of JNK by SP600125 reduces ischema/reperfusion injury in the rat lung and prolongs survival in rats after smoke inhalation injury (Ishii *et al*., 2004; Syrkina *et al*., 2007).

JNK has been implicated in nickel toxicity (Zhang *et al*., 2007); however, *in vitro* studies have not always been consistent (Samet *et al*., 1998; Tessier and Pascal, 2006). The signaling factors mediating nickel-induced JNK activation have remained elusive. At least 14 MAP3Ks, such as MAP3K1–4, are involved in mediating diverse upstream signals to the JNK pathway (Schlesinger *et al*., 1998), but it is not known which MAP3Ks are involved in transmitting the nickel signals. In the present work, we used genetically modified cells and mice to evaluate the role of two MAP3Ks, MAP3K1 and MAP3K2, in JNK activation and nickel-induced acute lung injury.

MATERIALS AND METHODS

Mice and exposure protocol. The *Map3k1*$^{\Delta KD/\Delta KD}$, also known as *Mekk1*$^{\Delta KD/\Delta KD}$, mice were described before (Zhang *et al*., 2003) and were backcrossed for at least seven generations into the C57/BL6 background. Intercrosses were carried out to generate *Map3k1*$^{+/\Delta KD}$ and *Map3k1*$^{\Delta KD/\Delta KD}$ mice. The wild-type C57/BL6 mice were purchased from Jackson Laboratory (Bar Harbor, ME). The *Map3k2*$^{+/-}$, also known as *Mekk2*$^{+/-}$, mice were described previously (Guo *et al*., 2002). All mice were maintained in the Experimental Animal Laboratory at the University of Cincinnati. Nickel aerosol (mass median aerodynamic diameter = 0.2 μm) was generated from 50mM $NiSO_4 \bullet 6H_2O$ (Sigma, St Louis, MO) and monitored as described previously (Wesselkamper *et al*., 2000). Mice were exposed to 150 ± 15 μg Ni^{2+}/m^3 in a 0.32-m^3 stainless steel inhalation chamber continuously, and survival time was recorded. The experimental procedures were approved by the University of Cincinnati Animal Care and Use Committee.

Cells, reagents, and antibodies. Mouse embryonic fibroblasts (MEFs) were prepared from E13.5 wild-type or mutant fetuses as described (Giroux *et al*., 1999) and were cultured in Dulbecco's modified Eagle's medium (DMEM) supplemented with 10% fetal bovine serum. All cell culture reagents were from Invitrogen (Carlsbad, CA). Nickel sulfate was from Sigma. Phospho-JNK antibody and X-gal were from Promega (Fitchburg, WI); antibodies for phospho-ERK and phospho-p38 were from Cell Signaling Technology (Danvers, MA); antibodies for β-actin, JNK, p38, and ERK were from Santa Cruz Biotechnology (Santa Cruz, CA), and anti-MAP3K1 was described previously (Xia *et al*., 2000).

Histology and X-gal staining. Whole-mount X-gal staining of wild-type, *Map3k1*$^{+/\Delta KD}$, and *Map3k2*$^{+/-}$ mice lung was performed as described previously (Zhang *et al*., 2003). In brief, whole lung was inflated with 4% paraformaldehyde (PFA) and isolated from mice, washed with cold phosphate buffer, and placed in PFA at 4°C for 20 min. Tissue was washed with cold phosphate buffer for three times, 5 min/each time, followed by washing in staining buffer containing 5mM $K_3Fe(CN)_6$, 5mM $K_4Fe(CN)_6$, 0.02% nonidet p40, 100mM $NaHPO_4$, pH 7.3, and 2mM $MgCl_2$ for 15 min. For staining, 1 mg/ml of X-gal was added to fresh staining buffer and incubated with tissue in the dark at 30°C overnight. Tissue was postfixed in 4% PFA overnight. For whole-mount examination, tissues were cleared by incubating serially in solutions containing 20, 50, 80, and 100% glycerol (vol/vol) brought to the final volume by 1% KOH (w/v). Each incubation step was carried out at 30°C and lasted 4–7 days. Pictures were taken using a Leica MZ16 F stereomicroscope with a ×0.5 plan objective. For histology, tissues were fixed in 4% PFA, dehydrated with a graded ethanol series, and embedded in paraffin. Tissues were serially sectioned at 4 μm and counterstained with eosin. Pictures were taken at various magnifications under the microscope.

Cell treatment, tissue lysates, and Western blot analyses. Eighty percent confluent monolayers of MEFs were deprived of growth factors for 16–24 h to minimize the basal levels of MAPK phosphorylation. The cells were treated with serum-free DMEM in the presence or absence of various doses of nickel sulfate for 4 h. By the end of the treatment, cells were washed with ice-cold PBS twice and lysed on ice with "egg lysis buffer" (50mM Tris, pH 7.5, 0.1% nonidet p40, 120mM NaCl, 1mM EDTA, 6mM ethyleneglycol-bis(aminoethylether)-tetraacetic acid, 20mM NaF, 1mM sodium pyrophosphate, 30mM 4-nitrophenyl phosphate, 1mM benzamidine, one tablet of EDTA-free protease inhibitor cocktail per 25 ml of buffer). Cell lysates were incubated on ice for 10 min and frozen at −80°C until use. After thaw on ice, cell lysates were centrifuged at 13,500 rpm for 15 min, and total cellular proteins were collected in the supernatant. In total, 100 μg of cell and tissue lysates was resolved on SDS-polyacrylamide gel electrophoresis followed by Western blot detection using appropriate antibodies.

Cytotoxicity assay. Cell viability was assessed by 3-(4,5-dimethylthiazol-2-yl)-5-(3carboxymethoxyphenyl)-2-(4-sulfophenyl)-2H-tetrazolium (MTS) cytotoxicity assay, using CellTiter 96 AQ_{ueous} One Solution (Promega, Madison, WI). Briefly, cells were seeded into 96-well plates at 1.5×10^4 cells per well and were cultured overnight. The cells were treated with $NiSO_4$ at different concentrations in serum-free medium for 10 h. CellTiter 96 AQ_{ueous} One Solution (20 μl per 100 μl medium) was added into each well, and cells were incubated at 37°C for 1–4 h. The absorbance (490 nm) was measured, and cell survival ratios were calculated as the ratio of absorbance in treated cells versus that in untreated cells. At least four wells were tested on each treatment condition in a single experiment, and the data from three independent experiments were used for statistical analyses.

Colony formation assay. MEFs were seeded at 2×10^3 cells per 6-cm tissue culture dishes and were maintained in the growth medium containing 1μM nickel sulfate. On day 7, the cells were washed with PBS and the colonies were stained for 2 min by 0.3% crystal violet (in 25% ethanol). The colonies on each plate were counted; the average numbers in the total of 10 plates under each treatment condition were calculated and were used for statistical analyses.

RESULTS

MAP3K1 Ablation Enhances JNK Activation by Nickel

To investigate the potential involvement of the MAP3Ks in MAPK activation, we examined nickel-induced MAPK phosphorylation in wild-type MEFs and MEFs deficient in MAP3K1, MAP3K2, or both. When exposed to increasing concentrations (1–50mM) of nickel, there was a dose-dependent induction in the phosphorylation of JNK, ERK,

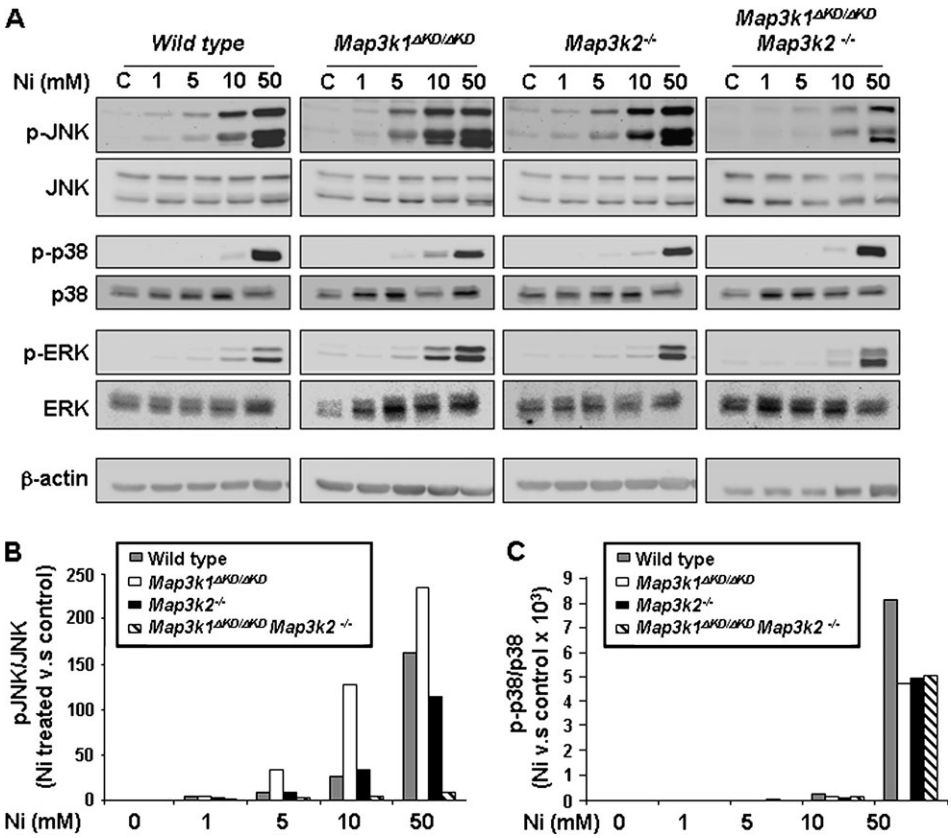

FIG. 1. The roles of MAP3K1 and MAP3K2 in nickel-induced JNK phosphorylation. Wild-type, *Map3k1*$^{\Delta KD/\Delta KD}$, *Map3k2*$^{-/-}$ and *Map3k1*$^{\Delta KD/\Delta KD}$*Map3k2*$^{-/-}$ mouse embryo fibroblasts were exposed to various concentrations of $NiSO_4$ as indicated for 4 h. (A) The cell lysates were subjected to Western blotting using the antibodies indicated. The ratio of (B) pJNK/total JNK and (C) pp38/total p38 was calculated following quantification by gel documentation system, and the fold induction was derived from comparing the ratio in treated versus that in untreated cells.

and p38 in all the cells examined (Fig. 1A). The overall pattern of MAPK phosphorylation did not appear to be overtly altered by MAP3K1 and MAP3K2 deficiency; however, quantification showed that the levels of phospho-JNK induced by nickel were quite different in the various gene ablation cells. In comparison to wild-type cells, phospho-JNK was more abundant in *Map3k1*$^{\Delta KD/\Delta KD}$, unchanged in *Map3k2*$^{-/-}$, and markedly reduced in *Map3k1*$^{\Delta KD/\Delta KD}$/*Map3k2*$^{-/-}$ cells (Fig. 1B). The levels of phospho-p38 and phospho-ERK were not obviously affected by MAP3K1 and MAP3K2 ablation, and nickel exposure had no effect on the levels of JNK or β-actin expression (Figs. 1A and C and data not shown).

MAP3K1 Ablation Potentiates Nickel Cytotoxicity

To determine the involvement of MAP3K1 and MAP3K2 in nickel cytotoxicity, we exposed wild-type, *Map3k1*$^{\Delta KD/\Delta KD}$, *Map3k2*$^{-/-}$, and *Map3k1*$^{\Delta KD/\Delta KD}$*Map3k2*$^{-/-}$ MEFs to various concentrations of nickel for 10 h and measured cell survival by MTS cytotoxicity assay. Survival decreased more in *Map3k1*$^{\Delta KD/\Delta KD}$ cells than in wild-type and *Map3k2*$^{-/-}$ cells. Conversely, *Map3k1*$^{\Delta KD/\Delta KD}$/*Map3k2*$^{-/-}$ MEFs were more resistant to nickel cytotoxicity (Fig. 2A). By colony formation assay, we evaluated cytotoxicity by chronic exposure to low concentration (1μM) of nickel. Similar to its acute toxicity, nickel caused a marked reduction of the *Map3k1*$^{\Delta KD/\Delta KD}$ colonies, while the *Map3k2*$^{-/-}$ and *Map3k1*$^{\Delta KD/\Delta KD}$/*Map3k2*$^{-/-}$ cells were similar to the wild-type MEFs in colony formation. Taken together, our observations reveal a role for MAP3K1 in suppressing JNK activation and preventing nickel cytotoxicity; on the other hand, MAP3K1 and MAP3K2 together potentiate JNK activation and nickel cytotoxicity. In either case, there is a good correlation between the levels of JNK activation and cytotoxicity caused by nickel.

MAP3K1 and MAP3K2 Expression in Mouse Lung Tissues

The MAP3Ks display tissue and cell-type specificity in signal transduction, partly due to differential tissue distribution patterns (Schlesinger *et al*., 1998). To determine in which adult tissues MAP3K1 may be functionally important, we examined MAP3K1 expression in lysates of various mouse tissues. The highest levels of MAP3K1 expression were seen in the olfactory bulb, thymus, spleen, skin, and lung, less MAP3K1

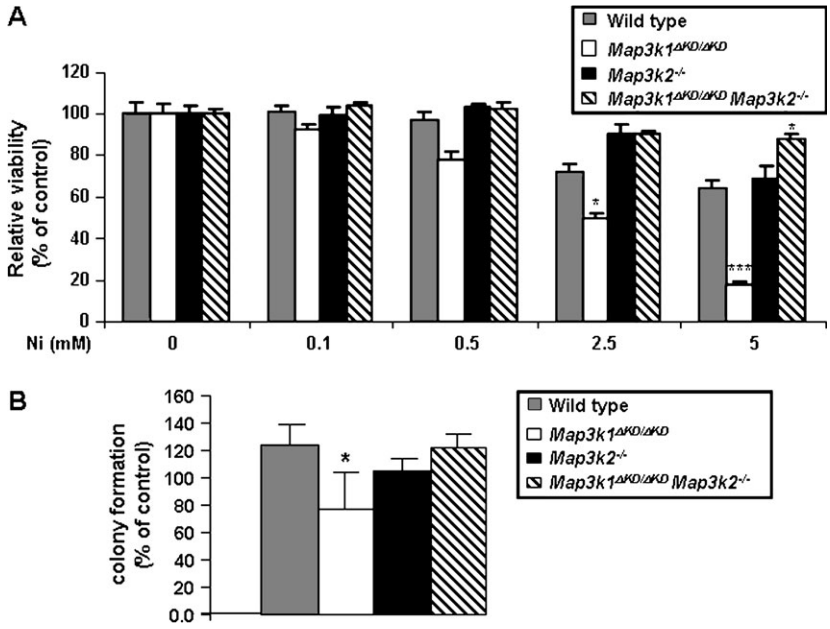

FIG. 2. The roles of MAP3K1 and MAP3K2 in nickel cytotoxicity. (A) Wild-type, *Map3k1*$^{\Delta KD/\Delta KD}$, *Map3k2*$^{-/-}$ and *Map3k1*$^{\Delta KD/\Delta KD}$*Map3k2*$^{-/-}$ mouse embryo fibroblasts were exposed to various concentrations of $NiSO_4$ as indicated for 10 h. Cell survival ratios were measured by MTS cytotoxicity assay. The MTS value in nickel-treated cells was compared to that of the untreated cells, and the relative cell survival rate was calculated. There are four samples in each treatment condition in each experiment, and results represent at least three independent experiments. (B) MEFs were grown in medium with or without $NiSO_4$ (1μM) for 7 days. The colonies were counted in 10 samples of each treatment condition. The average colonies in nickel-exposed conditions were compared to those in the control. Statistical analyses were done by student's *t*-test. $*p < 0.01$, $**p < 0.001$, and $***p < 0.0001$ were considered significantly different from the wild-type cells.

protein was detected in the cerebellum, heart, and testis, and none was observed in the kidney and liver (Fig. 3A). These results indicate that MAP3K1 protein is differentially expressed in mouse tissues and is highly expressed in the lung.

The *Map3k1*$^{\Delta KD}$ mice contain a *β-galactosidase* gene knocked in at the *Map3k1* locus such that β-gal expression is controlled by the endogenous *Map3k1* promoter (Xia *et al*., 2000), and as such the location of β-gal reflects *Map3k1* endogenous promoter activity. To further localize the MAP3K1-expressing cells, we performed whole-mount X-gal staining of the *Map3k1*$^{+/\Delta KD}$ mouse tissues followed by glycerol clarification procedures to identify the endogenous localization of the β-gal–positive, i.e., MAP3K1-expressing, cells. While no β-gal–positive cells were seen in the wild type, a distinct X-gal staining pattern was observed in the *Map3k1*$^{+/\Delta KD}$ mouse lung (Fig. 3B). Specifically, the β-gal–positive cells were located along the distal bronchi but not in the main stem bronchi or parenchyma of the lung. Further histological examination located the β-gal–positive cells to the bronchial epithelium and the wall of associated blood vessels, possibly in the smooth muscle cells (Fig. 3C). Very few, if any, MAP3K1-positive cells were present in the liver, consistent with nondetectable MAP3K1 proteins in this tissue by Western blotting (Fig. 3A). It was interesting to note that the *Map3k2*$^{+/-}$ mice, that also have a *β-galactosidase* gene knocked in (Guo *et al*., 2002), displayed β-gal–positive staining, i.e., *Map3k2* promoter activity, in the trachea, main stem bronchi, and distal bronchi of the lung, a pattern partially overlapping with that of *Map3k1* (Fig. 3B). The redundant and unique expression pattern of MAP3K1 and MAP3K2 suggests that these two MAP3Ks may play both common and cell-type–specific roles in the lung.

MAP3K1 Contributes to Protection against Nickel-induced Acute Lung Injury

Because MAP3K1 is abundantly expressed in the airway and is functionally involved in nickel cytotoxicity, we hypothesize that MAP3K1 may be involved in nickel-induced acute lung injury. To test this hypothesis, we exposed wild-type, *Map3k1*$^{+/\Delta KD}$ and *Map3k1*$^{\Delta KD/\Delta KD}$ mice to nickel and recorded survival time during exposure. Ablation of one functional *Map3k1* allele in *Map3k1*$^{+/\Delta KD}$ mice did not alter survival; however, *Map3k1* homozygous mutants died significantly sooner than wild-type mice (Fig. 4A). The mean survival time of the *Map3k1*$^{\Delta KD/\Delta KD}$ mice was shortened by 20 h relative to wild-type or *Map3k1*$^{+/\Delta KD}$ mice (Fig. 4B). During exposure, mice developed severe dyspnea, and gross pathology of the lung indicated air trapping and extensive hemorrhagic edema, supporting that lethality was a consequence of severe lung injury. We conclude that MAP3K1 expression and activity in the lung epithelium offer protection against nickel-induced lung injury.

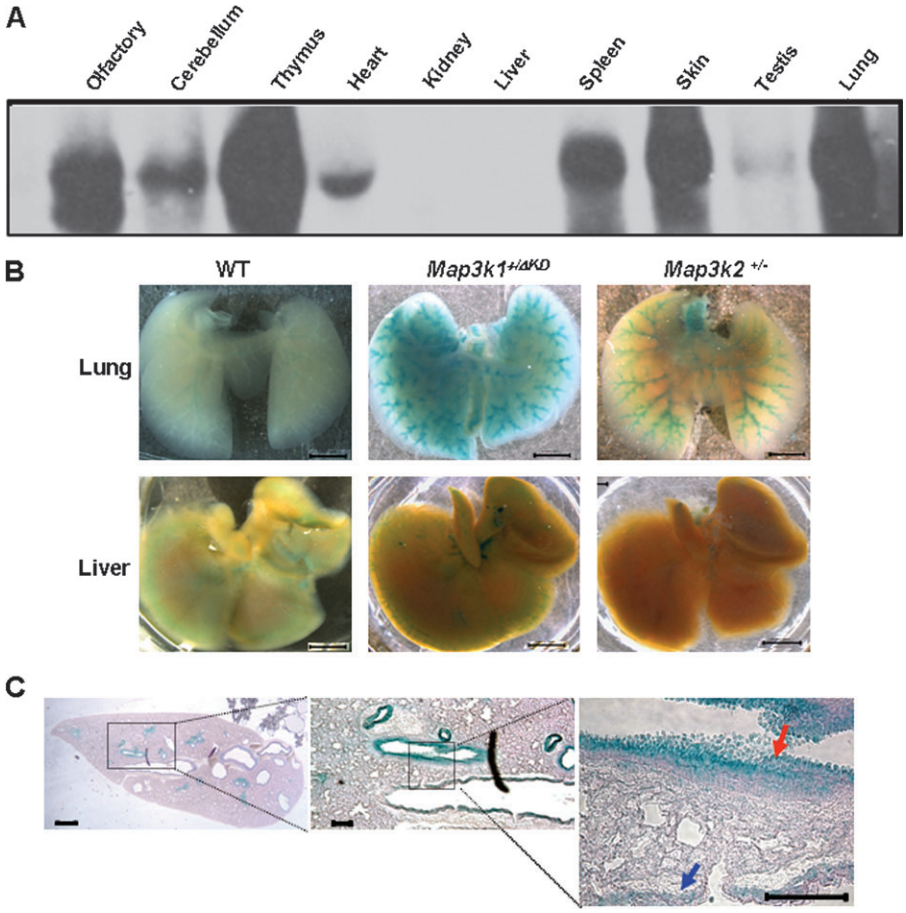

FIG. 3. MAP3K1 and MAP3K2 expression in mouse tissue. (A) Lysates of various mouse tissues as indicated were subjected to Western blotting using anti-MAP3K1. The results show differential MAP3K1 tissue distribution. (B) Lung and liver isolated from wild-type, *Map3k1*$^{+/\Delta KD}$ and *Map3k2*$^{+/-}$ mice were subjected to whole-mount X-gal staining, followed by tissue clarification procedures. Photographs were taken using a Leica MZ16 F stereomicroscope with a ×0.5 plan objective (total magnification ×5). Scale bar indicates 5000μM. X-gal staining (blue) is clearly positive in the airways of the *Map3k1*$^{+/\Delta KD}$ and *Map3k2*$^{+/-}$, but is absent in the wild-type mice. No staining was observed in the liver. (C) The X-gal–stained lungs isolated from the *Map3k1*$^{+/\Delta KD}$ mice were sectioned and processed with eosin staining. Photographs were taken at ×2 (left panel, scale indicates 40μM), ×10 (middle panel), and ×40 (right panel) with scale bars of 10μM. X-gal-positive–stained cells accumulate mainly at the airway epithelium (red arrow) and blood vessel (blue arrow).

DISCUSSION

Activation of signaling pathways is considered to be critical for acute lung injury; however, only a few *in vivo* studies have addressed which signaling factors are involved in the process. In previous studies, we have found that ablation of metallothionein-nitric oxide signaling (Wesselkamper *et al.*, 2006) and macrophage stimulating 1 receptor (c-met-related tyrosine kinase) (McDowell *et al.*, 2002) increases susceptibility to nickel-induced acute lung injury in mice. Conversely, transgenic expression of transforming growth factor α (Hardie *et al.*, 2002) and keratinocyte growth factor 7 (Tichelaar *et al.*, 2007) decreases susceptibility to nickel-induced acute lung injury in mice. Here, we have identified MAP3K1 as one of the targets that could be augmented to reduce acute lung injury because MAP3K1 ablation reduces mean survival time. MAP3K1 protein is expressed in mouse lung in the airway epithelium and blood vessel; its ablation therefore likely impairs the ability of the airway to counteract nickel toxicity.

MAP3K2, another MAP3K sharing similar activities with MAP3K1 in downstream pathway induction, is also highly expressed in the airway epithelium (Fanger *et al.*, 1997; Schlesinger *et al.*, 1998). It is possible that MAP3K1 and MAP3K2 are functionally redundant at least in some cells; therefore, lacking MAP3K1 causes only a 20% increase in lethality to the *Map3k1*$^{\Delta KD/\Delta KD}$ mice during nickel exposure. Studies using MEFs, however, suggest that MAP3K2 may be dispensable for cytotoxicity because *Map3k2*$^{-/-}$ cells do not differ from wild-type cells in response to nickel treatment. Interestingly, when both MAP3K1 and MAP3K2 are ablated, the *Map3k1*$^{\Delta KD/\Delta KD}$*Map3k2*$^{-/-}$ compound mutant cells are resistant to cytotoxicity. It is worth noting that molecular responses taking place in fibroblasts may not be quite the same as those in lung epithelial cells; hence, the precise role of

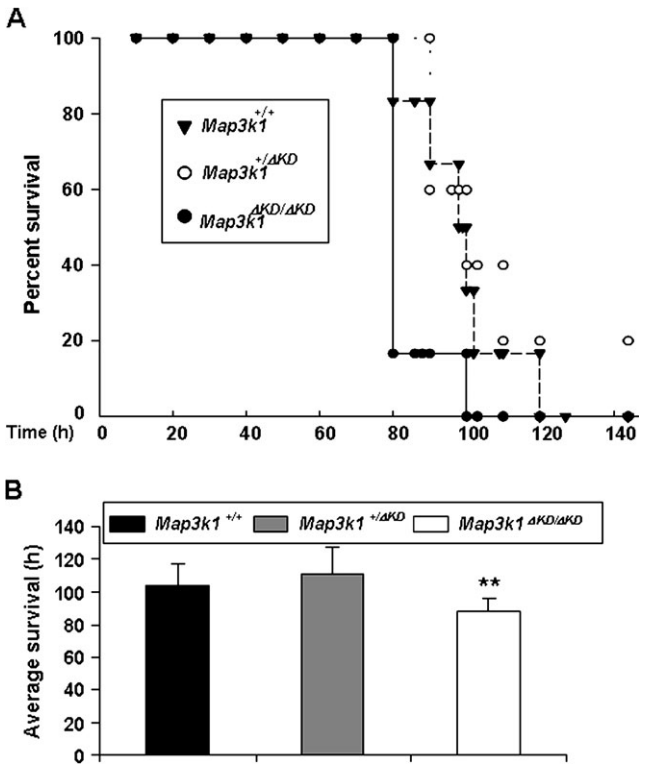

FIG. 4. MAP3K1 ablation decreased survival of mice during nickel-induced acute lung injury. (A) Wild-type, *Map3k1*$^{+/\Delta KD}$ and *Map3k1*$^{\Delta KD/\Delta KD}$ mice ($n = 6$ in each group) were exposed to 150 μg Ni/m^3 nickel (0.2-μm mass median aerodynamic diameter) continuously, and time of death was recorded. (B) The mean survival time of *Map3k1*$^{\Delta KD/\Delta KD}$ mice was significantly less than the wild-type control (**$p < 0.01$ as determined by student's *t*-test).

MEKK2 in nickel-induced acute lung injury may have to be evaluated *in vivo*.

In vitro, cell survival is inversely related to phospho-JNK levels in response to nickel; however, this relationship is complex. In comparison to wild-type cells, the *Map3k1*$^{\Delta KD/\Delta KD}$ cells display higher JNK activation and reduced survival, whereas the *Map3k1*$^{\Delta KD/\Delta KD}$*Map3k2*$^{-/-}$ cells have lower JNK activation and are resistant to cytotoxicity. This observation is consistent with the notion that JNK activity is promoting cell death (Faris *et al*., 1998; Lin and Dibling, 2002). Such a role would be consistent with the increase in survival noted in other models of acute lung injury when JNK phosphorylation is inhibited pharmacologically (Ishii *et al*., 2004; Syrkina *et al*., 2007). In addition to its well-established roles in transcription factor activation (Davis, 2000), JNK has recently been shown to mediate epigenetic histone modification in response to nickel (Ke *et al*., 2008). It is hence reasonable to suggest that the JNK pathway activation by nickel may potentiate lung injury by the way of activating gene expression.

At this time, we cannot explain why the *Map3k1*$^{\Delta KD/\Delta KD}$ cells differ from the *Map3k1*$^{\Delta KD/\Delta KD}$*Map3k2*$^{-/-}$ cells in regard to nickel-induced JNK activation. A likely scenario may be that nickel induces the JNK pathway through several MAP3Ks, including MAP3K1, MAP3K2, and others, and only when multiple members of the MAP3Ks are ablated, as in the *Map3k1*$^{\Delta KD/\Delta KD}$*Map3k2*$^{-/-}$ cells, there will be an obvious suppression of JNK activation. Furthermore, MAP3K1 may have additional negative feedback roles in downregulation of the JNK pathway; thus, *Map3k1*$^{\Delta KD/\Delta KD}$ cells, lacking such negative inhibition, will display more abundant JNK activation during nickel exposure. A role of MAP3K1 in inhibiting its downstream pathways has been described before (Lu *et al*., 2002; Witowsky and Johnson, 2003); this function is mediated through the plant homeodomain domain located at the N-terminus of MAP3K1, which acts as an E3 ubiquitin ligase that catalyzes downstream signaling factors for degradation.

Taken together, our studies suggest that there is a complex molecular interplay between MAP3K1 and MAP3K2 in the signal transduction pathways responding to nickel exposure. The MAP3K1 exhibits an unexpected role in suppressing nickel-induced JNK activation and reducing cytotoxicity. Hence, pharmacological agents that increase MAP3K1 activity may be useful in the treatment of nickel-induced acute lung injury happening in an occupational setting.

FUNDING

NIH (ES11798 to Y.X., ES15675 and HL063700 to G.L.); NIEHS Center for Environmental Genetics P30 Grant (ES06096) (University of Cincinnati).

ACKNOWLEDGMENTS

We thank Alvaro Puga for a critical reading of the manuscript.

REFERENCES

Antonini, J. M., Lewis, A. B., Roberts, J. R., and Whaley, D. A. (2003). Pulmonary effects of welding fumes: Review of worker and experimental animal studies. *Am. J. Ind. Med.* **43**(4), 350–360.

Boisleve, F., Kerdine-Romer, S., Rougier-Larzat, N., and Pallardy, M. (2004). Nickel and DNCB induce CCR7 expression on human dendritic cells through different signalling pathways: Role of TNF-alpha and MAPK. *J. Invest. Dermatol.* **123**(3), 494–502.

Chang, L., Jones, Y., Ellisman, M. H., Goldstein, L. S., and Karin, M. (2003). JNK1 is required for maintenance of neuronal microtubules and controls phosphorylation of microtubule-associated proteins. *Dev. Cell* **4**(4), 521–533.

Chen, N., Nomura, M., She, Q. B., Ma, W. Y., Bode, A. M., Wang, L., Flavell, R. A., and Dong, Z. (2001). Suppression of skin tumorigenesis in c-Jun NH(2)-terminal kinase-2-deficient mice. *Cancer Res.* **61**(10), 3908–3912.

Davis, R. J. (2000). Signal transduction by the JNK group of MAP kinases. *Cell* **103**(2), 239–252.

Dong, C., Yang, D. D., Wysk, M., Whitmarsh, A. J., Davis, R. J., and Flavell, R. A. (1998). Defective T cell differentiation in the absence of Jnk1. *Science* **282**(5396), 2092–2095.

Fanger, G. R., Johnson, N. L., and Johnson, G. L. (1997). MEK kinases are regulated by EGF and selectively interact with Rac/Cdc42. *EMBO J* **16**(16), 4961–4972.

Faris, M., Kokot, N., Latinis, K., Kasibhatla, S., Green, D. R., Koretzky, G. A., and Nel, A. (1998). The c-Jun N-terminal kinase cascade plays a role in stress-induced apoptosis in Jurkat cells by up-regulating Fas ligand expression. *J. Immunol.* **160**(1), 134–144.

Geiser, T., Jarreau, P. H., Atabai, K., and Matthay, M. A. (2000). Interleukin-1beta augments in vitro alveolar epithelial repair. *Am. J. Physiol. Lung Cell. Mol. Physiol.* **279**(6), L1184–L1190.

Giroux, S., Tremblay, M., Bernard, D., Cardin-Girard, J. F., Aubry, S., Larouche, L., Rousseau, S., Huot, J., Landry, J., Jeannotte, L., *et al*. (1999). Embryonic death of Mek1-deficient mice reveals a role for this kinase in angiogenesis in the labyrinthine region of the placenta. *Curr Biol* **9**(7), 369–372.

Guo, Z., Clydesdale, G., Cheng, J., Kim, K., Gan, L., McConkey, D. J., Ullrich, S. E., Zhuang, Y., and Su, B. (2002). Disruption of Mekk2 in mice reveals an unexpected role for MEKK2 in modulating T-cell receptor signal transduction. *Mol. Cell Biol.* **22**(16), 5761–5768.

Han, B., Lodyga, M., and Liu, M. (2005). Ventilator-induced lung injury: Role of protein-protein interaction in mechanosensation. *Proc. Am. Thorac. Soc.* **2**(3), 181–187.

Han, Z., Chang, L., Yamanishi, Y., Karin, M., and Firestein, G. S. (2002). Joint damage and inflammation in c-Jun N-terminal kinase 2 knockout mice with passive murine collagen-induced arthritis. *Arthritis Rheum.* **46**(3), 818–823.

Hardie, W. D., Prows, D. R., Piljan-Gentle, A., Dunlavy, M. R., Wesselkamper, S. C., Leikauf, G. D., and Korfhagen, T. R. (2002). Dose-related protection from nickel-induced lung injury in transgenic mice expressing human transforming growth factor-alpha. *Am. J. Respir. Cell Mol. Biol.* **26**(4), 430–437.

Ishii, M., Suzuki, Y., Takeshita, K., Miyao, N., Kudo, H., Hiraoka, R., Nishio, K., Sato, N., Naoki, K., Aoki, T., *et al*. (2004). Inhibition of c-Jun NH2-terminal kinase activity improves ischemia/reperfusion injury in rat lungs. *J. Immunol.* **172**(4), 2569–2577.

Ke, Q., Li, Q., Ellen, T. P., Sun, H., and Costa, M. (2008). Nickel compounds induce phosphorylation of histone H3 at serine 10 by activating JNK-MAPK pathway. *Carcinogenesis* (in press).

Kheradmand, F., Folkesson, H. G., Shum, L., Derynk, R., Pytela, R., and Matthay, M. A. (1994). Transforming growth factor-alpha enhances alveolar epithelial cell repair in a new in vitro model. *Am. J. Physiol.* **267**(6 Pt 1), L728–L738.

Kuan, C. Y., Yang, D. D., Samanta Roy, D. R., Davis, R. J., Rakic, P., and Flavell, R. A. (1999). The Jnk1 and Jnk2 protein kinases are required for regional specific apoptosis during early brain development. *Neuron* **22**(4), 667–676.

Li, L. F., Yu, L., and Quinn, D. A. (2004). Ventilation-induced neutrophil infiltration depends on c-Jun N-terminal kinase. *Am. J. Respir. Crit. Care Med.* **169**(4), 518–524.

Lin, A., and Dibling, B. (2002). The true face of JNK activation in apoptosis. *Aging Cell* **1**(2), 112–116.

Lippmann, M., Ito, K., Hwang, J. S., Maciejczyk, P., and Chen, L. C. (2006). Cardiovascular effects of nickel in ambient air. *Environ. Health Perspect.* **114**(11), 1662–1669.

Lu, Z., Xu, S., Joazeiro, C., Cobb, M. H., and Hunter, T. (2002). The PHD domain of MEKK1 acts as an E3 ubiquitin ligase and mediates ubiquitination and degradation of ERK1/2. *Mol. Cell* **9**(5), 945–956.

McDowell, S. A., Mallakin, A., Bachurski, C. J., Toney-Earley, K., Prows, D. R., Bruno, T., Kaestner, K. H., Witte, D. P., Melin-Aldana, H., Degen, S. J., *et al*. (2002). The role of the receptor tyrosine kinase Ron in nickel-induced acute lung injury. *Am. J. Respir. Cell Mol. Biol.* **26**(1), 99–104.

Sabapathy, K., Kallunki, T., David, J. P., Graef, I., Karin, M., and Wagner, E. F. (2001). c-Jun NH2-terminal kinase (JNK)1 and JNK2 have similar and stage-dependent roles in regulating T cell apoptosis and proliferation. *J. Exp. Med.* **193**(3), 317–328.

Sakashita, A., Nishimura, Y., Nishiuma, T., Takenaka, K., Kobayashi, K., Kotani, Y., and Yokoyama, M. (2007). Neutrophil elastase inhibitor (sivelestat) attenuates subsequent ventilator-induced lung injury in mice. *Eur. J. Pharmacol.* **571**(1), 62–71.

Samet, J. M., Graves, L. M., Quay, J., Dailey, L. A., Devlin, R. B., Ghio, A. J., Wu, W., Bromberg, P. A., and Reed, W. (1998). Activation of MAPKs in human bronchial epithelial cells exposed to metals. *Am. J. Physiol.* **275**(3 Pt 1), L551–L558.

Schlesinger, T. K., Fanger, G. R., Yujiri, T., and Johnson, G. L. (1998). The TAO of MEKK. *Front. Biosci.* **3**(6), 1181–1186.

Scott, L. K., Grier, L. R., Arnold, T. C., and Conrad, S. A. (2002). Respiratory failure from inhalational nickel carbonyl exposure treated with continuous high-volume hemofiltration and disulfiram. *Inhal. Toxicol.* **14**(11), 1103–1109.

Speizer, F. E. (2000). Occupational and environmental lung diseases: An overview. *Environ. Health Perspect.* **108**(Suppl. 4), 603–604.

Syrkina, O. L., Quinn, D. A., Jung, W., Ouyang, B., and Hales, C. A. (2007). Inhibition of JNK activation prolongs survival after smoke inhalation from fires. *Am. J. Physiol. Lung Cell. Mol. Physiol.* **292**(4), L984–L991.

Tessier, D. M., and Pascal, L. E. (2006). Activation of MAP kinases by hexavalent chromium, manganese and nickel in human lung epithelial cells. *Toxicol. Lett.* **167**(2), 114–121.

Tichelaar, J. W., Wesselkamper, S. C., Chowdhury, S., Yin, H., Berclaz, P. Y., Sartor, M. A., Leikauf, G. D., and Whitsett, J. A. (2007). Duration-dependent cytoprotective versus inflammatory effects of lung epithelial fibroblast growth factor-7 expression. *Exp. Lung Res.* **33**(8), 385–417.

Timblin, C., BeruBe, K., Churg, A., Driscoll, K., Gordon, T., Hemenway, D., Walsh, E., Cummins, A. B., Vacek, P., and Mossman, B. (1998). Ambient particulate matter causes activation of the c-jun kinase/stress-activated protein kinase cascade and DNA synthesis in lung epithelial cells. *Cancer Res.* **58**(20), 4543–4547.

Wesselkamper, S. C., McDowell, S. A., Medvedovic, M., Dalton, T. P., Deshmukh, H. S., Sartor, M. A., Case, L. M., Henning, L. N., Borchers, M. T., Tomlinson, C. R., *et al*. (2006). The role of metallothionein in the pathogenesis of acute lung injury. *Am. J. Respir. Cell Mol. Biol.* **34**(1), 73–82.

Wesselkamper, S. C., Prows, D. R., Biswas, P., Willeke, K., Bingham, E., and Leikauf, G. D. (2000). Genetic susceptibility to irritant-induced acute lung injury in mice. *Am. J. Physiol. Lung Cell. Mol. Physiol.* **279**(3), L575–L582.

Witowsky, J. A., and Johnson, G. L. (2003). Ubiquitylation of MEKK1 inhibits its phosphorylation of MKK1 and MKK4 and activation of the ERK1/2 and JNK pathways. *J. Biol. Chem.* **278**(3), 1403–1406.

Xia, Y., Makris, C., Su, B., Li, E., Yang, J., Nemerow, G. R., and Karin, M. (2000). MEK kinase 1 is critically required for c-Jun N-terminal kinase activation by proinflammatory stimuli and growth factor-induced cell migration. *Proc. Natl. Acad. Sci. USA* **97**(10), 5243–5248.

Zhang, D., Li, J., Wu, K., Ouyang, W., Ding, J., Liu, Z. G., Costa, M., and Huang, C. (2007). JNK1, but not JNK2, is required for COX-2 induction by nickel compounds. *Carcinogenesis* **28**(4), 883–891.

Zhang, L., Wang, W., Hayashi, Y., Jester, J. V., Birk, D. E., Gao, M., Liu, C. Y., Kao, W. W., Karin, M., and Xia, Y. (2003). A role for MEK kinase 1 in TGF-beta/activin-induced epithelium movement and embryonic eyelid closure. *EMBO J* **22**(17), 4443–4454.